Russian Journal of Nonlinear Dynamics, 2020, vol. 16, no. 1, pp. 13–21.
Full-texts are available at http://nd.ics.org.ru
DOI: 10.20537/nd200102

NONLINEAR PHYSICS AND MECHANICS

MSC 2010: 37D05, 37D20, 37D45, 37M25, 82C32, 92B20

Some Lattice Models with Hyperbolic Chaotic Attractors

S. P. Kuznetsov

Examples of one-dimensional lattice systems are considered, in which patterns of different spatial scales arise alternately, so that the spatial phase over a full cycle undergoes transformation according to an expanding circle map that implies the occurrence of Smale–Williams attractors in the multidimensional state space. These models can serve as a basis for design electronic generators of robust chaos within a paradigm of coupled cellular networks. One of the examples is a mechanical pendulum system interesting and demonstrative for research and educational experimental studies.

Keywords: dynamical system, chaos, attractor, Smale – Williams solenoid, Turing pattern, pendulum, parametric oscillations, cellular neural network

1. Introduction

The uniformly hyperbolic attractors were introduced in the mathematical theory of dynamical systems due to Smale, Anosov, Sinai, and other researchers in the 1960s – 1970s [1]. Hyperbolic attractors are characterized by roughness or structural stability. In the context of physical or technical objects it implies insensitivity of the dynamical behavior to small variations in parameters, manufacturing imperfections, interferences, etc. which may be significant for possible applications [2]. It turned out, however, that hyperbolic chaos is not widespread in real-world systems, and its implementation requires special efforts.

Received May 28, 2019
Accepted September 02, 2019

This work was partially supported by the Russian Science Foundation grants nos. 17-12-01008 (Section 2) and 15-12-20035 (Section 3).

Sergey P. Kuznetsov
spkuz@yandex.ru
Udmurt State University,
ul. Universitetskaya 1, Izhevsk, 426034 Russia
Saratov Branch of Kotel'nikov's Institute of Radio-Engineering and Electronics of RAS
ul. Zelenaya 38, Saratov, 410019 Russia

Smale – Williams solenoid is the simplest representative of the hyperbolic chaotic attractors. Imagining an abstract discrete-time dynamical system, we assume that the evolution in one step transforms a certain torus region in such way that it experiences longitudinal stretching and tranversal compression, folds into a loop with the number of turns $M \geqslant 2$, and is placed inside the original torus. Under multiple repetitions, the number of turns tends to infinity, and the resulting object will have a transversal Cantor structure. The essential point is that the angular coordinate evolves according to the expanding circle map. For individual orbits on the attractor the dynamics are chaotic. For clarity, the above description appeals to the three-dimensional state space, but such attractors can occur in spaces of higher dimension too.

Physical examples of systems with attractors of Smale – Williams type can be constructed using oscillators residing in states of excitation and inhibition alternately, while the angular variable has a sense of the oscillator phase [3]. Another approach is based on the treatment of patterns arising in an active medium, say, for Turing structures or standing waves, and the angular variable is a spatial phase [4–6]. A disadvantage of the first approach is that it requires, as a rule, the use of rather complex external driving for parameter modulation, combining low-frequency and high-frequency components. Within the second approach, instead of high-frequency modulation a spatial nonhomogeneity is introduced, which is effortless. A disadvantage is the need of exploiting systems of infinite dimension of the state space, which complicates mathematical description and practical implementations.

What seems to be of interest is the application of the second approach for organizing hyperbolic chaos in finite-dimensional systems, namely, in lattices of cells, whose dynamics are governed by ordinary differential equations. In this respect, it is worth mentioning a paradigm of cellular neural networks (CNN) based on electronic components designed as arrays of cells arranged in space [7]. These systems were suggested, particularly, for parallel data processing, as an alternative to traditional computational approaches. As one of the directions, the application of CNN was considered for analog modeling of complex space-time dynamics including Turing structures, spiral patterns, turbulence.

This article discusses three models of one-dimensional cell arrays, which can inspire the design of CNN generating rough chaos.

2. Nonautonomous lattice system generating Turing patterns

The simplest nonautonomous lattice system can be obtained by spatial discretization of the model based on the Swift – Hohenberg equation [4], where the alternate excitation of long-wave and short-wave Turing patterns is provided. Replacing the spatial differentiation operator in the equation of Ref. [4] with a difference operator, we obtain

$$\dot{u}_j + 2\kappa^2(1-2\kappa^2)(u_{j+1} - 2u_j + u_{j-1}) + \kappa^4(u_{j+2} - 2u_j + u_{j-2}) = \\ = (A - 1 + \varepsilon\delta_j)u_j - u_j^3, \quad (2.1)$$

where u_j is the dynamical variable related to the jth spatial cell, and κ, A, ε are the parameters. The quantities δ_j define the spatial nonhomogeneity, the role of which will be explained below. Note that in the lattice a connection is involved not only between the nearest neighbors but also with the neighbors through one, with a certain ratio between the coupling coefficients.

Let the system be a ring chain with the number of cells $2N$. If the parameter κ is constant and $\varepsilon = 0$, then in the linear approximation the increment of the pattern with the wavenumber k is $\lambda = A - (1 - 4\kappa^2 \sin^2 \pi k/2N)^2$, and it is maximal at $\sin(\pi k/2N) = 1/2\kappa$.

In the ring with the periodicity condition $u_{j+2N} = u_j$, the wave number k should be an integer. For patterns of wave numbers $k = 1$ and $k = 3$ the maximal increment is achieved, respectively, at $\kappa_1 = \frac{1}{2}\sin\frac{\pi}{N}$ and $\kappa_3 = \frac{1}{2}\sin\frac{3\pi}{N}$. We will assume that in Eq. (2.1) the parameter is modulated in time with period T in such way that the alternate excitation of these patterns is provided:

$$\kappa(t) = \kappa(t + nT) = \begin{cases} \kappa_1,\ 0 \leqslant t < T/2, \\ \kappa_3,\ T/2 \leqslant t < T. \end{cases}$$

At the stage $\kappa = \kappa_1$, a pattern is formed with the wave number $k = 1$ and some spatial phase φ, i.e., $u \sim U_1\cos(\pi j/N + \varphi) + \widetilde{U}_3\cos(3\pi j/N + 3\varphi)$, where $U_1 \sim \sqrt{A}$. The third harmonic arises due to the presence of a cubic term and has a small amplitude $\widetilde{U}_3 \ll U_1$. After switching to $\kappa = \kappa_3$, the long-wave component $k = 1$ decays, but the system becomes unstable with respect to the excitation with $k = 3$. The initial stimulation of the short-wave pattern is provided by $\widetilde{U}_3$, so that it accepts a spatial phase of 3φ. At the end of the stage the pattern $u \sim U_3\cos(3\pi j/N + 3\varphi)$ takes place, with $U_3 \sim \sqrt{A}$. After the next switching, the third harmonic decays, but instability for the first harmonic gives rise to growth of its amplitude. The "germ" is the component with $k = 1$ provided by combination of the damping short-wave mode and the spatial distribution $\varepsilon\delta_j$. If the fourth harmonic dominates in δ_j, then, due to the term $\cos(4\pi j/N)\cos(3\pi j/N + 3\varphi) = \frac{1}{2}\cos(\pi j/N - 3\varphi) + \ldots$, the long-wave pattern arises, this time with the phase of -3φ. Thus, at each full modulation period, the spatial phase is transformed in accordance with a three-fold expanding circle map.

Taking into account that spatial distributions of u_j are determined by odd harmonics, we can consider a lattice of twice less number of cells N. To do so we simply replace the boundary conditions of periodicity by the condition of sign change: $u_{-1} = -u_{N-1}$, $u_N = -u_0$. One can use a stroboscopic description of the dynamics on a period of the modulation by the Poincaré map $\mathbf{X}_n = \mathbf{F}(\mathbf{X}_{n-1})$, where the state vector is $\mathbf{X}_n = (u_0, u_1, \ldots, u_{N-1})_{t=nT}$.

Figure 1a illustrates space-time dynamics in the lattice system with $N = 12$. Distributions of the values u_j are shown at the instants of the parameter switches depending on the spatial index. Although u_j relate to discrete nodes, the points are linked in the plot to visualize the patterns clearly. As is seen, the waveforms at each new stage of activity jump chaotically over the lattice length. It can be verified that the chaotic displacement of the patterns at successive stages corresponds to transformation of the spatial phases according to the triple expanding circle map. During numerical integration of the equations, at the end of each modulation period a spatial phase of the pattern is evaluated as $\varphi_n = \arg(u_0 + iu_{N/2})$, and the data are plotted in coordinates $(\varphi_{n-1}, \varphi_n)$, see Fig. 1b. Observe that one passage of the full interval for the preimage corresponds to a triple passage of the image in the opposite direction. Compression of the phase volume in other directions in the state space ensures existence of the Smale – Williams type attractor. Figure 1c shows a set of points $(u_0, u_{N/2})$ obtained by successive iterations of the stroboscopic Poincaré map. An enlarged fragment of the plot illustrates the transversal Cantor structure inherent to the solenoid.

The total number of Lyapunov exponents for the system is $N = 12$, however, to judge about the nature of the attractor and its fractal properties it is sufficient to evaluate only few larger exponents. Numerically, the first three exponents at the chosen parameters are $\Lambda_1 = 0.993$, $\Lambda_2 = -5.085$, $\Lambda_3 = -34.19$. The positive one is responsible for the instability of trajectories on the attractor and for chaotic nature of the dynamics. It is close to the value $\ln 3 \approx 1.0986$ associated with the expanding map for the angular variable. The remaining negative exponents

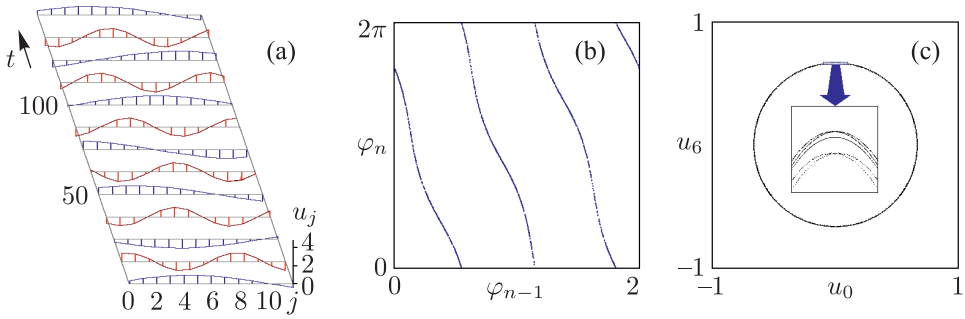

Fig. 1. (a) Evolution of patterns in the ring system (2.1) with the number of cells $N = 12$ and boundary condition of the sign change at the ends. The configurations relating to the parameter switching instants are shown. (b) Diagram of the spatial phase transformation on each one parameter modulation period. (c) Portrait of the attractor of the Poincaré map in projection on the plane. The parameters are: $A = 0.4$, $T = 25$, and $\varepsilon = 0.03$ with the spatial nonhomogeneity imposed with the dominated fourth harmonic: $\delta_j = \{0, 1, 1, 0, -1, -1, 0, 1, 1, 0, -1, -1\}$.

are responsible for the transverse compression and formation of the Cantor structure of the solenoid. Using the Kaplan – Yorke formula, one can estimate the fractal dimension of the solenoid as $D_{KY} = 1 + \Lambda_1/|\Lambda_2| \approx 1.20$.

3. Pendulum ring chain with vibrating suspension

A pendulum, the suspension point of which performs a periodic oscillatory motion in the vertical direction, is an interesting example of a mechanical system, where, depending on parameters, many different modes can be observed [8]. The phenomenology of dynamics becomes even richer if we turn to systems based on chains of coupled pendulums and to a continuous limit that is a medium described by the sine-Gordon equation [9].

Here we will consider a set of N pendulums suspended on a ring hoop, which is forced to perform a definite oscillatory motion in the vertical direction. Each pendulum is connected with the nearest neighbors by spiral springs, so that the moment of the interaction force is proportional to a relative deflection angle of the neighboring pendulums. Avoiding unnecessary complication of the model, we assume that dissipation is due to the presence of friction force between the hoop and the pendulums of moment proportional to the instantaneous angular velocity. The equations in dimensionless form are

$$\begin{gathered}(1 + \varepsilon\delta_j)\left[\ddot{\theta}_j + (1 + a(t))\sin\theta_j\right] = -\gamma\dot{\theta}_j + D(\theta_{j-1} - 2\theta_j + \theta_{j+1}), \\ j = 0, 1, \ldots, N-1,\end{gathered} \tag{3.1}$$

where θ_j is the deflection angle for the jth pendulum, γ is the dissipation parameter, D is the coupling coefficient of the neighboring pendulums, and $\varepsilon\delta_j$ is the relative deflection of the mass of the jth pendulum from the mean value. The ring arrangement of the pendulums implies imposition of the boundary conditions of periodicity: $\theta_{j+N} = \theta_j$.

Suppose the vertical movement imparted to the hoop to which the pendulums are suspended follows a sinusoidal law with amplitude A_2 and frequency ω_2 during N_2 oscillations, and then with amplitude A_1 and frequency ω_1 during N_1 oscillations, after which the switches are repeated

with period T:

$$a(t) = \begin{cases} A_2\omega_2^2 \sin\omega_2 t, \ 0 \leqslant t < \tau, \\ A_1\omega_1^2 \sin\omega_1(t-\tau), \ \tau \leqslant t < T, \end{cases} \qquad \tau = 2\pi\frac{N_2}{\omega_2}, \qquad T = 2\pi\left(\frac{N_2}{\omega_2} + \frac{N_1}{\omega_1}\right). \tag{3.2}$$

Bearing in mind that the eigenfrequencies of linear modes of oscillations of the ring chain of pendulums without taking into account pumping, dissipation and mass variation, are given by $\Omega_s = \sqrt{4D\sin^2\pi s N^{-1} + 1}$, we assign the pump frequencies ω_1 and ω_2 equal to twice the frequencies of the first and the third modes: $\omega_1 = 2\Omega_1$, $\omega_2 = 2\Omega_3$.

The dynamics may be treated in terms of the stroboscopic Poincaré map $\mathbf{X}_n = \mathbf{F}(\mathbf{X}_{n-1})$ transforming the $2N$-dimensional state vector $\mathbf{X}_n = (\theta_0, \theta_1, \ldots, \theta_{N-1}, \dot\theta_0, \dot\theta_1, \ldots, \dot\theta_{N-1})_{t=nT}$ for one period of the pump modulation.

The mechanism leading to the emergence of hyperbolic chaos is similar to that for the model of parametric excitation of oscillations of a nonlinear string of Ref. [5]. During pumping at the frequency ω_1 a standing wave is excited, for which we can write, roughly, $\theta_j \sim \sin(2\pi j/N + \varphi)$, where the phase constant φ depends on initial conditions. The amplitude stabilizes at some level due to nonlinearity of the pendulums. Also, because of the nonlinearity, there will be a component of the third spatial harmonic, having a spatial phase of 3φ. At the next stage, the pumping at ω_1 stops, and the oscillations of the first mode are damped. Now, however, pumping at frequency ω_2 is switched on, which leads to parametric instability for the standing wave of the third mode. This wave is formed from the initial perturbation given by the third spatial harmonic of the wave produced at the previous stage, so it will have the spatial phase shift of 3φ. Further, the stage of pumping at ω_1 comes again. The seed for the parametric oscillations growth is provided by a combination of the disturbance $\theta_j \sim \sin(6\pi j/N + 3\theta)$ left from the previous stage and the spatially nonuniform mass distribution given by δ_j. If it contains the dominating second harmonic $\delta_j \sim \sin(4\pi j/N)$, the combination contributing to the first mode has a spatial phase $\varphi_{\text{new}} = 3\varphi + \text{const}$, as $\sin(4\pi j/N)\sin(6\pi j/N + 3\theta) = \frac{1}{2}\cos(2\pi j/N + 3\theta) + \ldots$, and the parametrically excited standing wave will inherit the same phase. Thus, at each new modulation period, a three-fold expanding circle map for the phase takes place. The result of multiple repetition of the transformation will be the formation of the Smale – Williams solenoid in the state space of the map $\mathbf{X}_n = \mathbf{F}(\mathbf{X}_{n-1})$.

Figure 2a shows dependences of the angular accelerations of the pendulums on time according to data of numerical integration of (3.1) for sustained chaotic motion. Although pendulum oscillations themselves are indistinguishable on the scale of the graph, it shows clearly how the amplitudes vary in time in the system functioning in accordance with the mechanism described above. Panel 2b illustrates the transformation of the spatial phase of the standing waves during each modulation period of the pump. The phases $\varphi_n = \arg[\theta_0(nT) + i\theta_{N/4}(nT)]$ are calculated at the moments of switching the pump frequency from ω_1 to ω_2, when the first spatial mode is dominating. This diagram is the main evidence that the Smale – Williams type attractor indeed takes place since it demonstrates the required topological property. In the system under consideration, the solenoid is an object in the state space of the Poincaré map of dimension $2N = 24$. Panel 2c shows this attractor in two-dimensional projection. The enlarged fragment in the diagram visualizes the transverse structure of fibers of the solenoid.

The total number of Lyapunov exponents of the attractor of the Poincaré map is $2N = 24$. The first three exponents are $\Lambda_1 = 1.0913$, $\Lambda_2 = -2.484$, $\Lambda_3 = -14.70$. A positive exponent responsible for the chaotic nature of the dynamics is close to the value $\ln 3 \approx 1.0986$ associated with the threefold expanding map. The remaining exponents are negative, being responsible

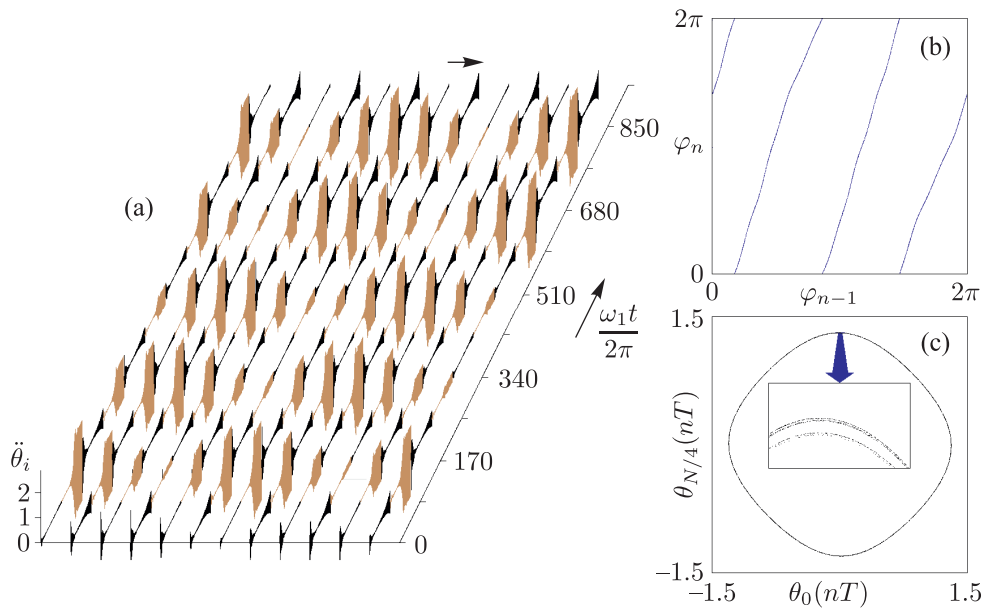

Fig. 2. (a) Diagrams of dependences of the angular accelerations of pendulums on time in the sustained chaotic mode based on the numerical solution of the differential equations, where the stages of slow and fast oscillations of the suspension are shown in brown and black. (b) Plot of the spatial phase transformation on each modulation period of pumping. (c) Portrait of the attractor of the Poincaré map in projection on the plane. The number of chain elements is $N = 12$, the parameters are $D = 1.19$ and $\gamma = 0.12$, $A_1\omega_1^2 = A_2\omega_2^2 = 0.6$. The variation of the masses is characterized by $\varepsilon = 0.01$ and a set $\delta_j = \{0, 1, 1, 0, -1, -1, 0, 1, 1, 0, -1, -1\}$. Switches of the pump frequencies between $\omega_1 = 2.297$ and $\omega_2 = 3.677$ take place after each $N_1 = 85$ and $N_2 = 136$ oscillations of the suspension.

for the transversal compression and formation of the Cantor structure of the solenoid of fractal dimension estimated from the Kaplan – Yorke formula as $D_{KY} \approx 1.44$.

4. Autonomous lattice system with hyperbolic chaos

In this section an autonomous lattice system is examined inspired by a distributed system with Smale – Williams attractor proposed in Ref. [6]. We change the spatial differentiation by finite-difference operators and add some modifications to adopt the model to simpler implementation. Consider a ring chain of $2N$ cells governed by the equations

$$\begin{aligned} \dot{u}_j &= D_0(u_{j-1} - 2u_j + u_{j-1}) + u_j^3 - u_j v_j^2 - \alpha u_{j+N} + \varepsilon\delta_j v_j, \\ \dot{v}_j &= (-\gamma + u_j^2)v_j + \mu u_j^2. \end{aligned} \tag{4.1}$$

Here u_j, v_j are the dynamic variables of the cells numbered by $j = 0, 1, \ldots, 2N-1$, and μ, ε, γ are the parameters. In addition to coupling of neighboring cells characterized by D_0, each cell is linked with the opposite element of the ring that is characterized by coefficient α. By a set of values δ_n, a weak spatial inhomogeneity is introduced.

If $\varepsilon = 0$, then, near the equilibrium state the substitution $u_j \sim \exp(\lambda t - i\pi kj/N)$ leads to expression for the increments of modes of wave numbers k, which, in accordance with the condition of periodicity, should be integers: $\lambda(k) = -\alpha(-1)^k - 4D_0 \sin^2(\pi k/2N)$. Assuming

$0 < \alpha < 4D_0 \sin^2(3\pi/2N)$, only one mode $k = 1$ has a positive increment, while the other modes are damped, including the homogeneous one with $k = 0$.

When specifying the spatial nonhomogeneity as the third spatial harmonic, i.e., $\delta_j \sim \cos 3\pi j N^{-1} + \ldots$, it is possible to ensure generation of the hyperbolic chaos.

Suppose the system is initially close to zero state and demonstrates growth in time of the spatial distribution u_j with the wave number $k = 1$. In the general case, this is a superposition of the sine and cosine components with some coefficients that can be written as a single term with some spatial phase φ: $u_j \sim \cos(\pi j N^{-1} + \varphi)$. When the factor $(-\gamma + u_j^2)$ in the second equation becomes positive, the growth of the variable v_j starts. Since at its initiation the process is stimulated by a quadratic term u_j^2, the spatial dependence of v_j will be determined by the second harmonic: $v_j \sim \cos^2(\pi j N^{-1} + \varphi) = \frac{1}{2} + \frac{1}{2}\cos(2\pi j N^{-1} + 2\varphi)$. As the values of v_j grow, the variables u_j start to decrease rapidly at some time due to the inhibitory effect of the term v_j^2 in the first equation. When the values u_j become small enough, the variables v_j also experience damping with decrement determined by γ. As a new stage of increase of u_j comes, it is stimulated by a term $\varepsilon\delta_j v_j$, namely, by its first harmonic: $\delta_j v_j \sim \cos(3\pi j/N)\cos(2\pi j/N + 2\varphi) = = \frac{1}{2}\cos(\pi j/N - 2\varphi) + \ldots$ This ensures transfer of the double phase with the opposite sign to the first harmonic of u_j: $\varphi_{\text{new}} \approx -2\varphi$.

Similar dynamics can be provided in a lattice of twice less number of cells. Indeed, as the distributions of u_j are determined by odd harmonics, and for v_j by even ones, the solutions of (4.1) we consider must satisfy $u_{j+N} = -u_j$ and $v_{j+N} = v_j$. Therefore, instead of (4.1) we can write the equations for N cells

$$\begin{aligned} \dot{u}_j &= D_0(u_{j-1} - 2u_j + u_{j+1}) + u_j^3 - u_j v_j^2 + \alpha u_j + \varepsilon\delta_j v_j, \\ \dot{v}_j &= (-\gamma + u_j^2)v_j + \mu u_j^2, \end{aligned} \tag{4.2}$$

where the boundary conditions of periodicity are replaced by conditions of sign change at the ends: $u_{-1} = -u_{N-1}$, $u_N = -u_0$. Here, unlike (4.1), the long-distance interactions are excluded; the respective term in the equation contains now the variable for the same cell with inverted sign.

The system (4.2) can also be described in terms of the Poincaré map, the dimension of which is $2N-1$. To do so, we need to introduce a cross-section in the state space of the system (4.2) by some hypersurface S, which is defined by some algebraic equation $f(u_0, v_0, \ldots, u_{N-1}, v_{N-1}) = 0$ and must cross the flow of phase trajectories. The Poincaré map expresses the vector of a point on the hypersurface through the vector of the previous its intersection by the trajectory: $\mathbf{X}_n = \mathbf{F}(\mathbf{X}_{n-1})$.

Figure 3 shows space-time diagrams illustrating the dynamics of the ring system (4.1) with the number of cells $2N = 12$. The distributions of the values u and v are shown depending on the spatial index j plotted along the horizontal axis at time instants corresponding to the maximal values of the first mode amplitude. As can be seen from the figure, the waveforms at each new stage of activity jump chaotically on the chain length.

Similar dynamics occur for the same parameters in the system (4.2) with the number of cells $N = 6$ with the boundary conditions of sign reversal at the ends, see Fig. 4. The chaotic displacement of the patterns at successive stages of activity corresponds to transformation of the spatial phases according to the double expanding circle map. In the process of numerical integration of the equations at the time of each mth maximum of the first mode amplitude evaluated as $\sqrt{u_0^2 + u_{N/2}^2}$, the spatial phase is calculated as $\varphi_n = \arg(u_0 + iu_{N/2})$, and the data are plotted in coordinates $(\varphi_{n-1}, \varphi_n)$, see panel 4b. Although the shape of the branches is distorted

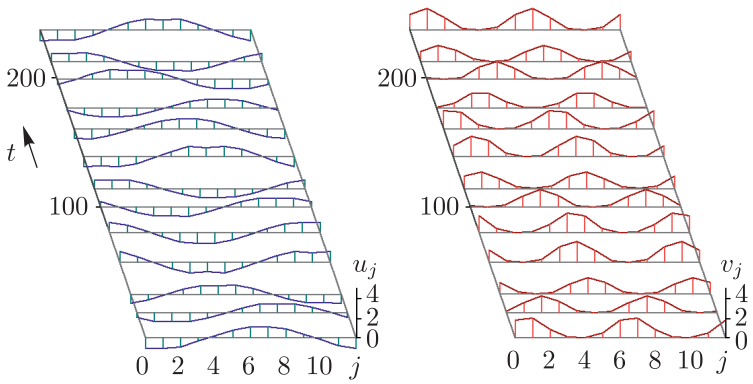

Fig. 3. Evolution of patterns in the ring system (4.1) with the number of cells $2N = 12$ in the sustained chaotic regime, on the left for the variable u, and on the right for the variable v. The configurations relating to successive maximums of the first mode amplitudes are shown. The parameters are: $D_0 = 8$, $\alpha = 2.2$, $\gamma = 0.6$, $\mu = 0.4$, $\varepsilon = 0.25$, $\delta_j = \{1, -1, -1, 1, 1, -1, -1, 1, 1, -1, -1, 1\}$.

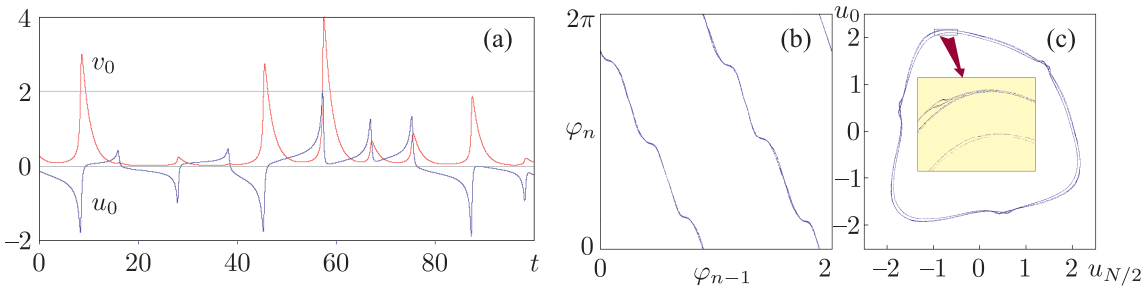

Fig. 4. Waveforms in the sustained regime of chaotic self-oscillations for a cell $j = 0$ in system (4.2) (a), diagram for the spatial phases (b) and attractor in the Poincaré section (c). The parameters are $D_0 = 8$, $\alpha = 2.2$, $\gamma = 0.6$, $\mu = 0.4$, $\varepsilon = 0.25$, $\delta_j = \{1, -1, -1, 1, 1, -1\}$.

in comparison with the ideal linear expanding circle map, this does not violate its affiliation to the same topological class. In the presence of the phase volume compression in other directions in the state space it ensures the occurrence of the Smale – Williams type attractor. Panel 4c shows a set of points $(u_0, u_{N/2})$ corresponding to the moments of maximal amplitudes of the first mode. This is a portrait of the attractor in the Poincaré section in a two-dimensional projection.

The total number of Lyapunov exponents for the system (4.2) is $2N = 12$. The computed first three exponents are $\lambda_1 = 0.0597$, $\lambda_2 = 0.0000$, $\lambda_3 = -0.2046$. As the average period of the Poincaré section passages is $T \approx 9.866$ according to the calculations, the largest Lyapunov exponent of the Poincaré map is 0.589, which roughly agrees with the value $\ln 2 \approx 0.693$. The second exponent is zero and refers to a perturbation along the reference trajectory in the autonomous system. The remaining exponents are negative. The Kaplan – Yorke dimension for the Poincaré map attractor is $D_{KY} = 1 + \lambda_1/|\lambda_3| \approx 1.29$, which reflects the fractal structure of the solenoid.

5. Conclusion

We have considered three lattice models in the form of one-dimensional arrays of coupled cells, which are able to generate hyperbolic chaos associated with attractors of Smale – Williams type. These examples show the possibility of implementing such attractors in finite-dimensional

systems, where the spatial phase of forming and disappearing patterns undergoing expanding circle map on a characteristic time interval plays the role of angular variable on Smale – Williams solenoids. It is to be hoped that the models can inspire the design of electronic generators of rough chaos, following the earlier suggested paradigm of coupled neural networks. One of the examples is a ring pendulum system, which seems to be an interesting and demonstrative mechanical model for research and educational experimental studies illustrating the hyperbolic chaos.

References

[1] *Dynamical Systems 9: Dynamical Systems with Hyperbolic Behaviour,* D. V. Anosov (Ed.), Encyclopaedia Math. Sci., vol. 66, Berlin: Springer, 1995.

[2] Elhadj, Z. and Sprott, J. C., *Robust Chaos and Its Applications,* World Sci. Ser. Nonlinear Sci. Ser. A Monogr. Treatises, vol. 79, Hackensack, N.J.: World Sci., 2011.

[3] Kuznetsov, S. P., Dynamical Chaos and Uniformly Hyperbolic Attractors: From Mathematics to Physics, *Phys. Uspekhi,* 2011, vol. 54, no. 2, pp. 119–144; see also: *Uspekhi Fiz. Nauk,* 2011, vol. 181, no. 2, pp. 121–149.

[4] Kuptsov, P. V., Kuznetsov, S. P., and Pikovsky, A., Hyperbolic Chaos of Turing Patterns, *Phys. Rev. Lett.,* 2012, vol. 108, no. 19, 194101, 4 pp.

[5] Isaeva, O. B., Kuznetsov, A. S., and Kuznetsov, S. P., Hyperbolic Chaos of Standing Wave Patterns Generated Parametrically by a Modulated Pump Source, *Phys. Rev. E,* 2013, vol. 87, no. 4, 040901(R), 4 pp.

[6] Kruglov, V. P., Kuznetsov, S. P., and Pikovsky, A., Attractor of Smale – Williams Type in an Autonomous Distributed System, *Regul. Chaotic Dyn.,* 2014, vol. 19, no. 4, pp. 483–494.

[7] Chua, L. O. and Roska, T., *Cellular Neural Networks and Visual Computing: Foundations and Applications,* Cambridge: Cambridge Univ. Press, 2002.

[8] Butikov, E. I., *Pendulum with Oscillating Suspension (60 Years of Kapitza Pendulum),* 2017 (Russian).

[9] *The sine-Gordon Model and Its Applications: From Pendula and Josephson Junctions to Gravity and High-Energy Physics,* J. Cuevas-Maraver, P. Kevrekidis, F. Williams (Eds.), Cham: Springer, 2014.